

Kinetic Antiferromagnetism in the Triangular Lattice

Jan O Haerter and B Sriram Shastry

Physics Department, University of California, Santa Cruz, Ca 95064

(November 21, 2018)

Abstract

We show that the motion of a single hole in the infinite U Hubbard model with frustrated hopping leads to weak metallic antiferromagnetism of kinetic origin. An intimate relationship is demonstrated between the simplest versions of this problem in 1 and 2 dimensions, and two of the most subtle many body problems, namely the Heisenberg Bethe ring in 1-d and the 2-dimensional triangular lattice Heisenberg antiferromagnet.

The role of kinetic energy in the theory of magnetism is crucial: while virtual processes promote antiferromagnetism in insulators, as in the theory of superexchange, real (or direct) kinetic processes usually promote ferromagnetism as a corollary of metallicity, as in the theory of double exchange [1,2]. The Nagaoka Thouless (NT) theorem [3,4] is of great importance in providing a rigorous mechanism for metallic ferromagnetism, notwithstanding the limitations of its context, that of a single hole in the limit of infinite repulsion. In this work we study the latter problem on certain 1-d and 2-d lattices with *electronic frustration*, a term defined by computing the sign of the hopping amplitudes around the smallest closed loop of a lattice, in complete parallel to the more familiar spin counterpart. If the sign is negative then the lattice is said to be electronically frustrated. The NT theorem applies only to the non frustrated cases, our focus is on the frustrated cases where not much is known reliably. We find surprisingly that in these cases the *real kinetic processes promote antiferromagnetism in the metallic phase*.

Our immediate motivation for studying electronically frustrated lattices is to understand the physics of systems such as the recently found sodium cobalt oxide system Na_xCoO_2 [5]. We present some analytical and numerical results for the one hole frustrated problem. Our main analytical tool is a novel reduction of the problem to an effective spin model, which yields insights into the physics. We have supplemented this with a numerical study using exact diagonalization of the effective spin problem, exploiting the symmetries of the clusters. Following the numerical work on the triangular lattice Heisenberg model (HM) by Bernu *et al* [6] we compute the exact eigenvalues in different total spin sectors for clusters of various sizes, and this leads to “towers of excitations”. These help one to distinguish between spin liquid states and various ordered states, something that variational studies cannot quite do [7]. Our findings are consistent with a three sublattice broken spin symmetric ground state, very similar to that of the triangular lattice HM [6,8]

We study periodic clusters of the infinite U Hubbard model with L sites and $N = L - 1$ particles with $H = - \sum_{i,j,\sigma} t_{i,j} c_{\vec{R}_j,\sigma}^\dagger c_{\vec{R}_i,\sigma}$, where $c_{\vec{R}_i,\sigma}$ are Gutzwiller projected fermions with single occupancy constraint built into them. Due to the periodicity, we may define a wave

vector \vec{k} for each wave function, and consider the action of H in a fixed \vec{k} subspace. Let us locate the hole at site \vec{R}_{i_0} , and write a basis state $|\alpha\rangle = c_{\vec{R}_1, \sigma_{\vec{R}_1}}^\dagger c_{\vec{R}_2, \sigma_{\vec{R}_2}}^\dagger \dots c_{\vec{R}_N, \sigma_{\vec{R}_N}}^\dagger |0\rangle$. A generic state may be written as $\psi(\vec{k}, \alpha) = \frac{1}{\sqrt{L}} \sum_{\vec{r}} e^{i\vec{k} \cdot \vec{r}} T_{\vec{r}} |\alpha\rangle$, where $T_{\vec{r}}$ is a (spatial) translation operator $T_{\vec{r}} c_{\vec{R}_i, \sigma}^\dagger T_{\vec{r}}^\dagger = c_{\vec{R}_i + \vec{r}, \sigma}^\dagger$. Exploiting the translation invariance of the Hamiltonian, the matrix element of H in such a state is expressible in terms of an effective \vec{k} dependent operator

$$\langle \beta | H_{eff}^{\vec{k}} | \alpha \rangle = \sum_{\vec{\delta}} t_{\vec{\delta}} e^{-i\vec{\delta} \cdot \vec{k}} \langle \beta | T_{\vec{\delta}} c_{\vec{R}_{i_0} - \vec{\delta}, \sigma}^\dagger c_{\vec{R}_{i_0}, \sigma}^\dagger | \alpha \rangle. \quad (1)$$

In this frame of reference, we hold the hole at a fixed site, as the entire set of spins flows past it. While this reduction is suggestive, it is not yet equivalent to finding an effective *spin* exchange representation, since the translation operators carry the complexity of fermionic negative signs. We can make considerable progress in specific problems as follows.

1-dimension: Let us first consider the general 1-d case with arbitrary range of hopping t_r . Let the hole reside at the L th site, so that the $L - 1 = N$ particles occupy sites $1 \rightarrow N$ with some spin configuration $|\sigma_1, \dots, \sigma_N\rangle = c_{1, \sigma_1}^\dagger c_{2, \sigma_2}^\dagger \dots c_{N, \sigma_N}^\dagger |0\rangle$. Operating with terms in H shifting the hole to its left, we find $t_{L,j} (-1)^{(L-j)} c_{1, \sigma_1}^\dagger \dots c_{j-1, \sigma_{j-1}}^\dagger c_{j+1, \sigma_{j+1}}^\dagger \dots c_{N, \sigma_N}^\dagger c_{L, \sigma_j}^\dagger |0\rangle$. We next restore the hole to the L th site from the j th site, so we need to translate by $r = L - j$ units. This gives rise to negative signs that can be calculated readily, and the answer written down in terms of the permutation operator $P_{i,j} = \frac{1}{2} + 2\vec{S}_i \cdot \vec{S}_j$, and *spin translation operator* $\mathcal{T} = P_{1,2} P_{2,3} \dots P_{N-1,N}$ acting as a cyclic permutation on a lattice of length N as

$$H_{eff}^k = \sum_r (-1)^{r(L-r)} (t_r e^{-ikr} P_{r, r+1} \dots P_{2,3} P_{1,2} (\mathcal{T})^r + hc).$$

The sum is over the range of hopping, thus the spin problem is defined on a periodic ring of length N rather than $L = N + 1$. In the simplest frustrated case we consider a model with nearest and second neighbor hopping $t_1 = t$, $t_2 = t'$, with both $t, t' > 0$. This (railroad trestle) lattice may be considered a strip of the triangular lattice. For this case, and with L odd, the effective Hamiltonian is

$$H_k^{t,t'} = t e^{-ik} \mathcal{T} + t' e^{-2ik} P_{1,2} (\mathcal{T})^2 + hc, \quad (2)$$

the full spectrum is obtained by varying k . The hole has been eliminated, and we arrive at an impurity bond model residing on the deleted $L - 1$ site lattice. The first term of Eq(2) bodily translates all spin configurations, hence all spin states remain degenerate. The second term discriminates between the configurations through the single exchange term $P_{1,2}$.

The ground state of Eq(2) was found numerically for rings up to $L = 19$. L is taken to be odd to allow for the possibility of singlet ground states, and indeed in all cases, the ground state is a singlet [9]. The correlation functions are found by imposing pbc's with length N [10]. These alternate in sign and seem to decay as a power law for small t'/t , changing to a faster and possibly exponential decay at large t'/t . This behavior is reminiscent of that of the HM with a second neighbor interaction, $H_h = J_1 \sum_n \vec{S}_n \cdot \vec{S}_{n+1} + J_2 \sum_n \vec{S}_n \cdot \vec{S}_{n+2}$. Here it is known [11] that the Bethe point $J_2 = 0$ has power law decay along with a logarithmic correction to the correlations so that asymptotically $C(r) \equiv \frac{1}{N} \sum_{i=1,N} \langle \vec{S}_i \cdot \vec{S}_{i+r} \rangle = (-1)^r \left\{ \frac{A}{|r|} + \frac{B(\log|r|)^{\frac{1}{2}}}{|r|} \right\} + O(1/r^2)$ [10]. The logarithmic term arises from the umklapp term, and B varies with J_2 within a power law phase persisting upto $J_2^*/J_1 \sim .24$ beyond which there is a gap in the spectrum. To compare with this behavior, we compute the structure function $g(y, t') = \sum_{r=1}^N (-1)^r C(r)$. Plotted as a function of $y = \log N$ in the power law phase, it is expected to be a sum of two terms, one $\sim y$ from A, and another $\sim y^{\frac{3}{2}}$ from the logarithmic term B. For various values of t' we show g as function of y in Fig(1). We also display the corresponding structure functions on the same lattice sizes for the nn HM ($J_2 = 0$) and the Haldane Shastry (HS) model [12] which has $B = 0$. It is clear that the small t'/t cases are very similar to the Heisenberg model, whereas the case of t'/t large appear to be gapped. We note that in the limit $t' \rightarrow 0^+$, the structure function g approaches the corresponding value for the HM. Remarkably enough, the individual correlation functions $C(r)$ approach those for the nn HM to the available precision (6 decimal places)! Taking a closer look, we studied the wave functions for small clusters (upto $L=13$). We found that the ground state of the impurity model, when translated as $\sum_r \exp(iPr)(\mathcal{T})^r |\text{impurity gs} \rangle$ with an appropriate (Marshall sign) momentum $P=0$ (π) for $N/2$ even (odd), becomes *the exact ground state of the Heisenberg model*. Based on these results we conjecture that the

$t' \rightarrow 0^+$ impurity model ground state after translation becomes the Bethe ground state of the Heisenberg ring. Finite t' seems related to further ranged exchange on a smaller scale than t' (i.e. $o(t')$). We thus find that the impurity spin model may be regarded loosely as the HM, with a scaled down exchange $J^{eff} = t'/N$ to make meaningful comparisons of energetics.

The Triangular Lattice In 2-dimensions the effective Hamiltonian Eq(1) can again be reduced to a spin operator. Let us imagine a two dimensional rhomboidal lattice with N_1 columns and M_1 rows ($L = N_1 M_1$) and the topology of a torus. We consider a particular term where the hole has hopped to the site $\vec{R}_{i_0} - \vec{\delta}_i$, and the translation is along $\vec{\delta}_i$ so as to restore the hole to the fixed site \vec{R}_{i_0} . It is enough to consider half the $\vec{\delta}_i$'s corresponding to forward hops, the back hops contribute to the hermitean conjugate. The translation is expressible as a specific permutation of the $L - 1 = (N_1 M_1 - 1)$ variables \vec{R}_l written in some specific order. This permutation can be decomposed into c_i cycles, each of length l_m so that $\sum_m l_m = L - 1$. The translation operator $T_{\vec{\delta}_i}$ accumulates phase factors of $(-1)^{l_m - 1}$ from each cycle relative to the pure spin translation operator $\mathcal{T}_{\vec{\delta}_i}$, and one extra minus sign arises from the row containing the hole, so that the overall phase factor is $-(-1)^{\sum_m (l_m - 1)} = (-1)^{L - c_i}$, and hence

$$H_{eff}^k = \sum_i \{t_{\vec{\delta}_i} (-1)^{L - c_i} e^{-i\vec{k} \cdot \vec{\delta}_i} \mathcal{T}_{\vec{\delta}_i} + h.c.\}. \quad (3)$$

For the triangular lattice we note that $\vec{\delta} = \hat{x}$ gives $c_i = M_1$ i.e. the number of rows, $\vec{\delta} = \frac{1}{2}\hat{x} + \frac{\sqrt{3}}{2}\hat{y}$ gives $c_i = N_1$ i.e. the number of columns. In the case of the third hop $\vec{\delta} = -\frac{1}{2}\hat{x} + \frac{\sqrt{3}}{2}\hat{y}$, c_i depends upon the relative prime-ness of N_1 and M_1 but is trivial to compute for any given cluster once and for all. The translations \mathcal{T} act only on the spin labels, and satisfy $\mathcal{T}_{\vec{\delta}_i} c_{\vec{R}, \sigma_{\vec{R}}}^\dagger \mathcal{T}_{\vec{\delta}_i}^\dagger = c_{\vec{R}, \sigma_{\vec{R} + \vec{\delta}_i}}^\dagger$ for $\vec{R} \neq \vec{R}_0 + \vec{\delta}_i$, and $\mathcal{T}_{\vec{\delta}_i} c_{\vec{R}_0 + \vec{\delta}_i, \sigma_{\vec{R}_0 + \vec{\delta}_i}}^\dagger \mathcal{T}_{\vec{\delta}_i}^\dagger = c_{\vec{R}_0 + \vec{\delta}_i, \sigma_{\vec{R} - \vec{\delta}_i}}^\dagger$, i.e. is a unit spin translator along the $\vec{\delta}_i$ direction for all sites except the one nearest to the hole where it shifts by two units.

To gain insight into the type of magnetic ordering in the triangular lattice we have performed exact diagonalization of small clusters [13]. We exploit the translation and rotation invariance by working with the deleted lattice in the subspace with $S_z = 0$. We also use

time reversal invariance so that under a global transformation $\sigma_j \rightarrow -\sigma_j$, its eigenvalues are $\kappa = \pm 1$. We find that if $(L - 1)/2$ is odd (even) the even spin states have $\kappa = -1(1)$, the odd spin states the opposite value.

We contrast systems either supporting or frustrating 3-sublattice order. In particular, we choose systems of 9, 21 and 27 sites which support 3-sublattice order [13]. The 3×3 -cluster displays high spatial symmetry which is reflected by a 7-fold degenerate ground state, one of which is a singlet which lies in the $(\mathbf{k} = 0, \kappa = 1)$ -sector. Due to its small size and geometry, in this cluster, every nearest neighbor (nn) is also a second neighbor and the third neighbor is the site itself. Thus, 3-sublattice order is forced by the boundary conditions in this cluster. We found a vanishing of the fluctuation of the operator $Q = \sum_{\langle i,j \rangle} (\vec{S}_i \cdot \vec{S}_j - n_i n_j / 4)$ in the singlet ground state. This curious result implies that within the tJ-model, both the contributions to the Hamiltonian share a common ground state for this cluster. In terms of the deleted lattice, the ground state of H_{eff} is exactly the ground state of the nn HM. Next, we compute the spectra of the 21 and 27 site clusters. We found that the states corresponding to $\vec{k} = \vec{0}$ or $\vec{Q}^* \equiv \frac{4\pi}{3}\hat{x}$ were found to be lower in energy and nearly degenerate. This can be attributed to a unit cell tripling, as one expects in case of 3-sublattice order. We find in Fig(2) a systematic behavior of the excitations, in close parallel to those for the triangular lattice HM [6]. One can define a “moment of inertia” [6] I as the inverse of the slope of the line joining the bottoms of the different S_{tot} towers of excitations. Our moment of inertia $I \sim L^2$ as compared to the Heisenberg value $\sim L$, again understandably in view of the extensivity of the latter model, and suggests $J_{eff} \sim t/L$. A noteworthy feature is the striking “subgap” in each tower, this separates the ground state from the excitations that start out sparsely and then seem to form a continuum. A very similar feature in the HM has been identified with the magnons [6] with an energy scale $\omega = c|k| \sim 1/\sqrt{L}$, and seems equally relevant here. In the 21-site cluster the states corresponding to three vectors k_1, k_2 and k_3 are all very close in energy. This can be understood in terms of a 1st BZ diminished in size by 1/3 as these three momentum vectors are placed in equal distances from the corners of this new 1st BZ. In the 27-site cluster, the picture is very similar. Again, the $\vec{k} = \vec{0}$ or \vec{Q}^*

states are clearly separated from the rest of the spectrum. The family of first excited states is constituted by the momenta k_1 , k_3 and k_4 , which are now vectors that lie exactly on the corners of the diminished 1st BZ. In this cluster, a second family of excited states emerges, which is populated by states belonging to the k_2 subspace. This vector lies in the center of the neighboring diminished 1st BZ in y-direction of k_0 . This point corresponds to a state of half the wave-number of the classical Néel state and is the least 'compatible' with the 3-sublattice scenario, thus leading to the highest excitation energy.

We also studied system of 15 and 21 sites, which frustrate the three sublattice order through their particular choice of boundary conditions [13]. We found that the energies of the frustrated clusters are considerably higher than for the unfrustrated ones. For 21 sites we can compare these directly: they are respectively -4.08577 and -4.18233 , thereby showing the clear preference for three sublattice order. In plot (c) of Figure(2) we compare the tower of states obtained for this frustrated 21 site cluster. The regular features described above are now perturbed, the zero-momentum states no longer constitute the ground states of the different spin sectors and the quasi-degeneracy can no longer be identified. This scenario is similar to that obtained by a HM with an additional 4-site ring exchange term [14].

We also calculated the structure function $S(\vec{q}) = \sum_{i,j} \exp(i\vec{q} \cdot (\vec{r}_i - \vec{r}_j)) < \vec{S}_i \cdot \vec{S}_j > / L$. It is useful to identify $v = \sqrt{S(\vec{Q}^*)/(L+6)}$ as the physical order parameter, with the same normalizations as in the HM [6]. The clusters compatible with 3-sublattice order contain the wave vector \vec{Q}^* -value, unlike the frustrated clusters. While the compatible clusters show a clear peak for $S(\vec{Q}^*)$, the frustrated clusters still show a peak at the \mathbf{q} -vector closest to \vec{Q}^* . Thus, 3-sublattice order is likely to be dominant in arbitrary systems and is not an artifact of a biased choice of boundary conditions. For the compatible systems we plot in the inset of Fig. (1) v vs. $L^{-1/2}$. and compare with results for the HM obtained in [6], normalizing to the maximum possible value of $S(\vec{Q}^*)$. Extrapolation to infinite system size suggests a substantial finite intercept (~ 0.849). This shows strong similarities with the studies on the HM [6], and suggests Néel long range order originating solely from the motion of a single hole in a spin background.

In Fig (1 inset) we also plot the ground state energy. The small system size and high symmetry of the 9 site cluster leads to a fairly large ground state energy while the 21 and 27 site clusters appear to show rapid convergence, we estimate $E_{gs} = -4.183 \pm 0.005$. On the square lattice, this swift convergence has also been observed by Poilblanc et al. [15]. Finally, the impurity model allows us to study the nature of the *spin texture* surrounding the hole [13]. In the (unfrustrated) hexagon surrounding the hole, we find substantial alternating antiferromagnetic order $\langle \vec{S}_i \cdot \vec{S}_j \rangle \approx -0.34$ similar in magnitude and nature to that observed for a HM on a square lattice [16]. This local impurity-order rapidly transitions into three-sublattice antiferromagnetic correlations at greater distances from the hole. Thus, the hole can be seen as a moving impurity around which spins tend to line up antiferromagnetically.

In conclusion, we have argued for *kinetic antiferromagnetism* on frustrated lattices. The preference for antiferromagnetism arises from the subtle phase dependence of the kinetic motion. Hole hopping mimics the effect of antiferromagnetic exchange energy, with the scale of a single impurity exchange bond per hole. The remarkable mapping to the Bethe ring in 1-d and close similarity with the HM on triangular lattice highlight this subtle phenomenon. Our effect should be most prominent in situations where superexchange is negligible. At least qualitatively used, as in Ref [17], our findings can thus be interpreted as leading to *weak antiferromagnetism* with $J_{eff} \sim +cx|t|$ in the case of the frustrated lattices, where x is the hole concentration.

ACKNOWLEDGMENTS

This work was supported by nsf-dmr 0408247. We are grateful to O. Cépas, Z. Fisk and A. P. Young for helpful comments.

REFERENCES

- [1] C. Zener, Phys. Rev. 82 403 (1951), For a recent review see M. Salamon and M. Jaime, Rev Mod Phys **73** 582 (2001).
- [2] P. W. Anderson, Phys. Rev. 79, 350 (1950).
- [3] Y. Nagaoka, Phys Rev. **147**, 392 (1966).
- [4] D. J. Thouless, Proc Phys Soc (London) **86**, 893 (1965).
- [5] B. G. Levi, Physics Today, Search and Discovery, **56**,15 (2003).
- [6] B. Bernu et al, Phys. Rev. **B 50** 10048 (1994); P. Lecheminant et al, Phys. Rev. **B 56**,2521 (1997).
- [7] S. V. Iordanskii and A. V. Smirnov, Sov Phys JETP **52**, 981 (1981). Their best estimate of energy is $-4.07|t|$.
- [8] D. A. Huse and V. Elser, Phys. Rev. Letts. **60**,2531 (1988) , S. Liang, B. Doucot and P. W. Anderson, Phys. Rev. Letts **61** ,365 (1988).
- [9] The ground state occurs at $k = 0$ for $L=3,7,11..$ and at $k = \pi$ for $L=5,9,13...$ Strictly speaking $k = \pi$ is not allowed in these cases, we therefore insert an appropriate flux in the ring to shift the momenta.
- [10] The Hubbard correlations actually peak at a wave vector different from π by terms of $O(1/L)$ due to the slight doping. The correlations functions found by imposing PBC's of length N are more systematic, peak exactly at π and differ from those of the Hubbard case by known terms of $O(1/L)$.
- [11] R. Jullien and F. D. M. Haldane, Bull Am Phys Soc,**28**, 344 (1983); I. Affleck *et al* et al, J. Phys. A. **22**, 511 (1989); R. Singh, M. E. Fisher and R. Shankar, Phys Rev **B 39**, 2562 (1989); R. Chitra *et al*, Phys. Rev. **B 52**, 6581 (1995).
- [12] F. D. M. Haldane Phys. Rev. Letts. **60**, 635 (1988), B. S. Shastry **60**, 639 (1988).

- [13] Figures depicting all the clusters used are available at <http://physics.ucsc.edu/~sriram/clusters.pdf>. These are reproduced here as Supplementary figures (3-7). Certain clusters frustrate 3-sublattice order while others are compatible with this order.
- [14] G. Misguich et al, Phys Rev **B 60** 1064 (1999).
- [15] D. Poilblanc et al, Phys Rev **B 46** 6435 (1992).
- [16] J. D. Reger and A. P. Young, Phys. Rev. **B 37**, 5978 (1988).
- [17] P. W. Anderson *et al* J. Phys. Cond. Mat. **16** R755 (2004) argue in the ferromagnetic context for a doping induced NT weakening of the superexchange in the pseudo gap phase of High Tc systems $J_{eff} = J - cx|t|$.

FIGURES

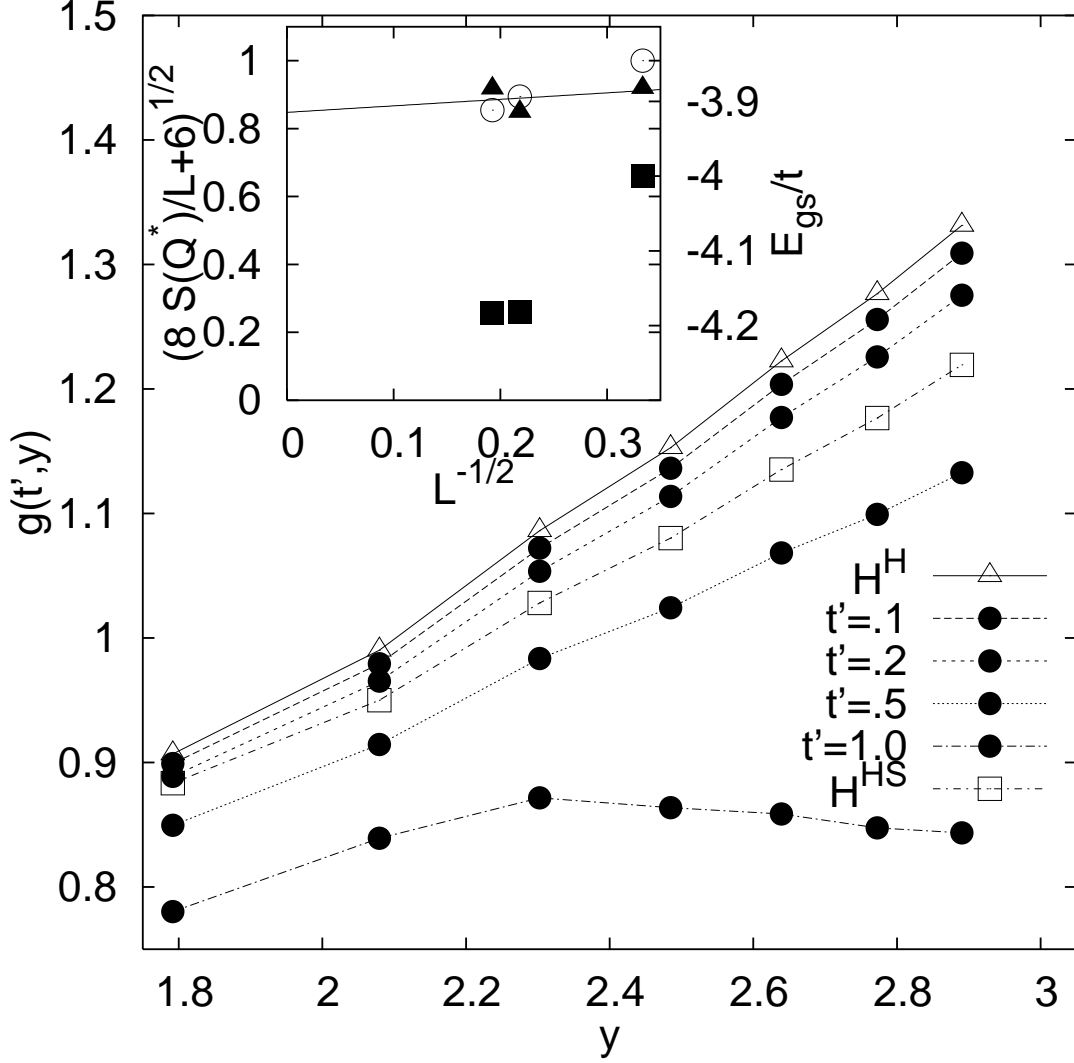


FIG. 1. 1-d structure function $g(y, t')$ of $H^{t, t'}$ for various t' compared to Heisenberg (H^H) and Haldane-Shastry (H^{HS}) model. In the limit $t' \rightarrow 0$, $H^{t, t'}$ correlations converge to those of H^H . **Inset:** 2-d: Size dependence of the structure function on 2-d triangular lattice for Hubbard and Heisenberg [6] models denoted by solid triangles and open circles. The solid squares are the ground state energy of H_{eff}

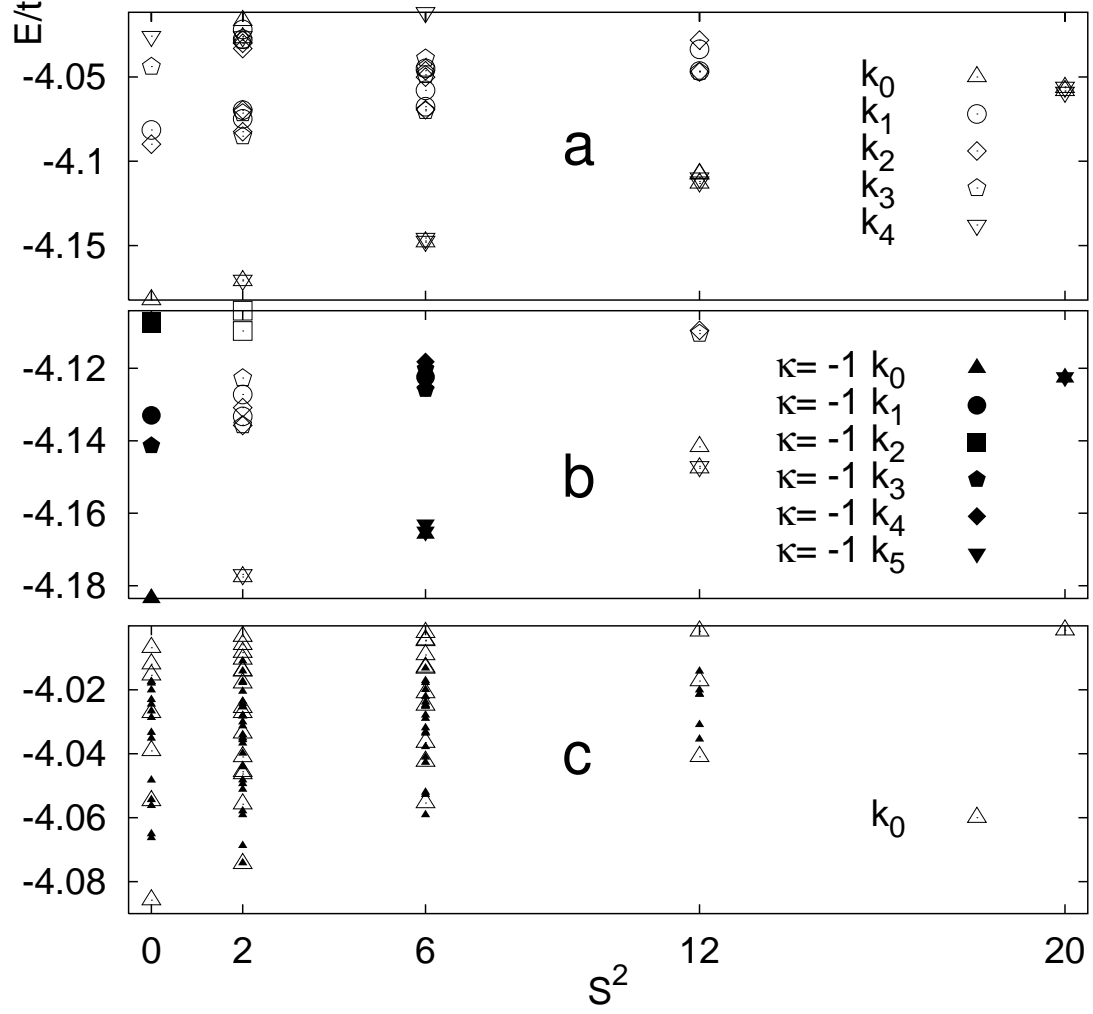


FIG. 2. a (b): Clusters with 21 (27) sites. Symbols correspond to different subspaces: k - momentum eigenvalue numbered in increasing magnitude of k , b: solid (open) symbols correspond to $\kappa = -1$ ($\kappa = 1$) c: The frustrated 21 site cluster, zero momentum states ($k_0 = 0$) emphasized

3 sublattice-order preserving clusters

Distinct colors correspond to different sublattices.

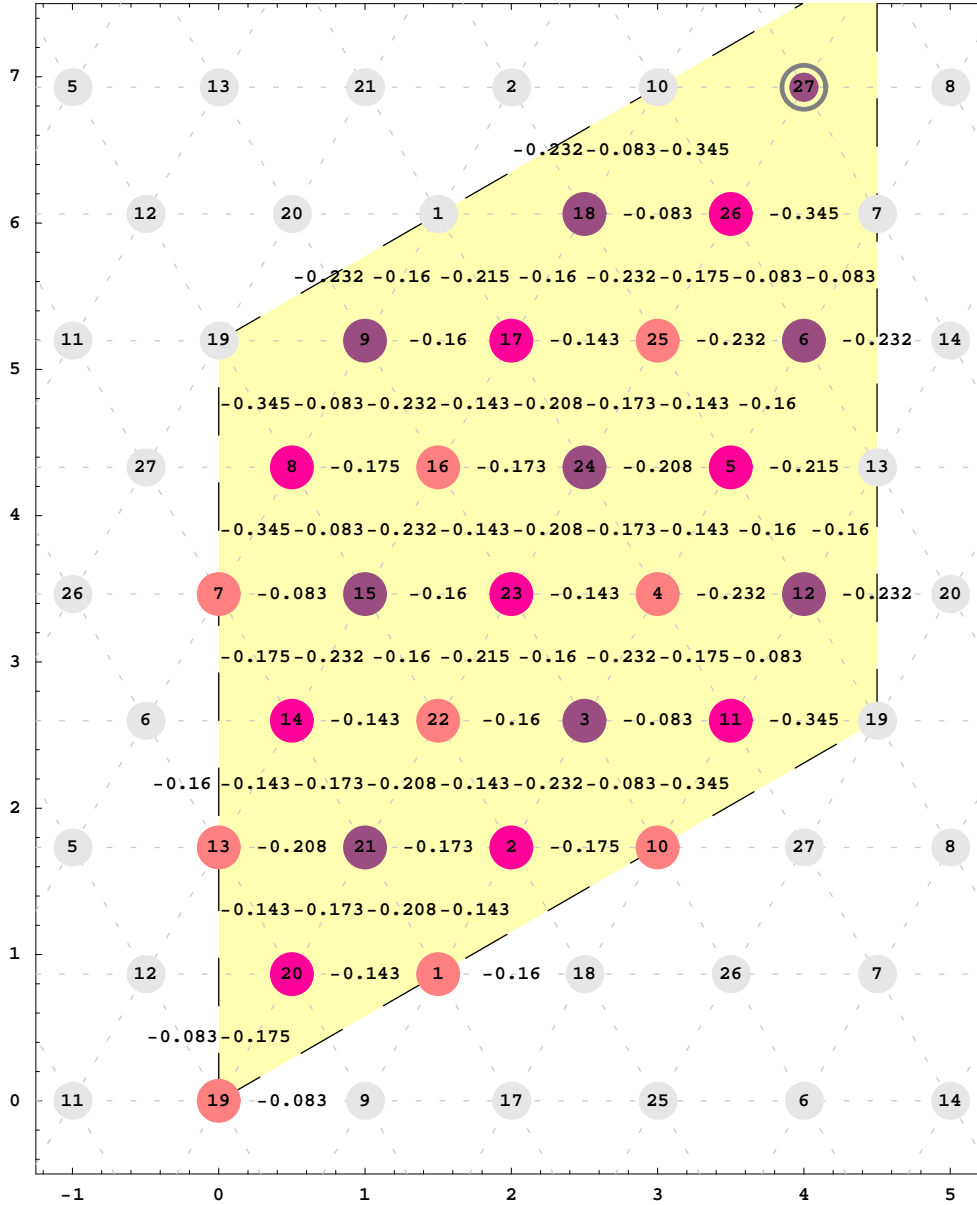


FIG. 3. The largest (27 site) cluster used in our exact diagonalizations: localized hole on site 27, decimal numbers between site i and j show correlation function $\langle S_i \cdot S_j \rangle$, note behavior of correlation function on hexagon surrounding the hole

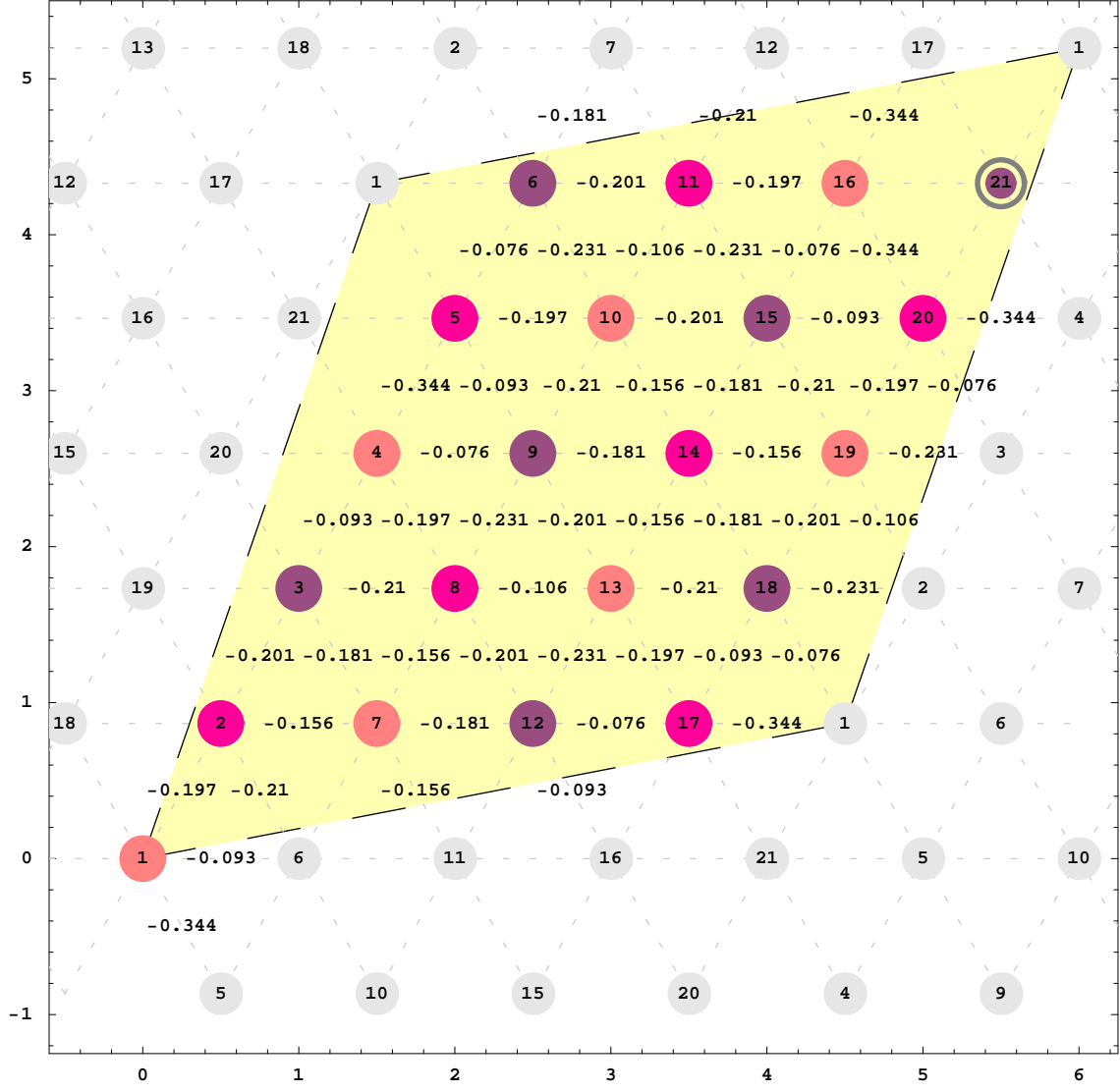
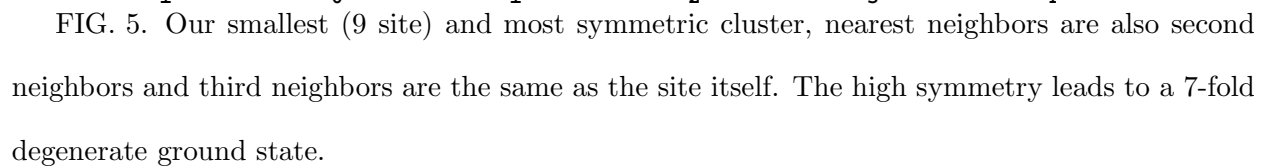


FIG. 4. The 21 site cluster. Note that this cluster maps onto a 1D ring with hoppings t_1 , t_4 and t_5 by moving along the directions of numbered sites and using periodic boundary conditions



3 sublattice-order frustrating clusters

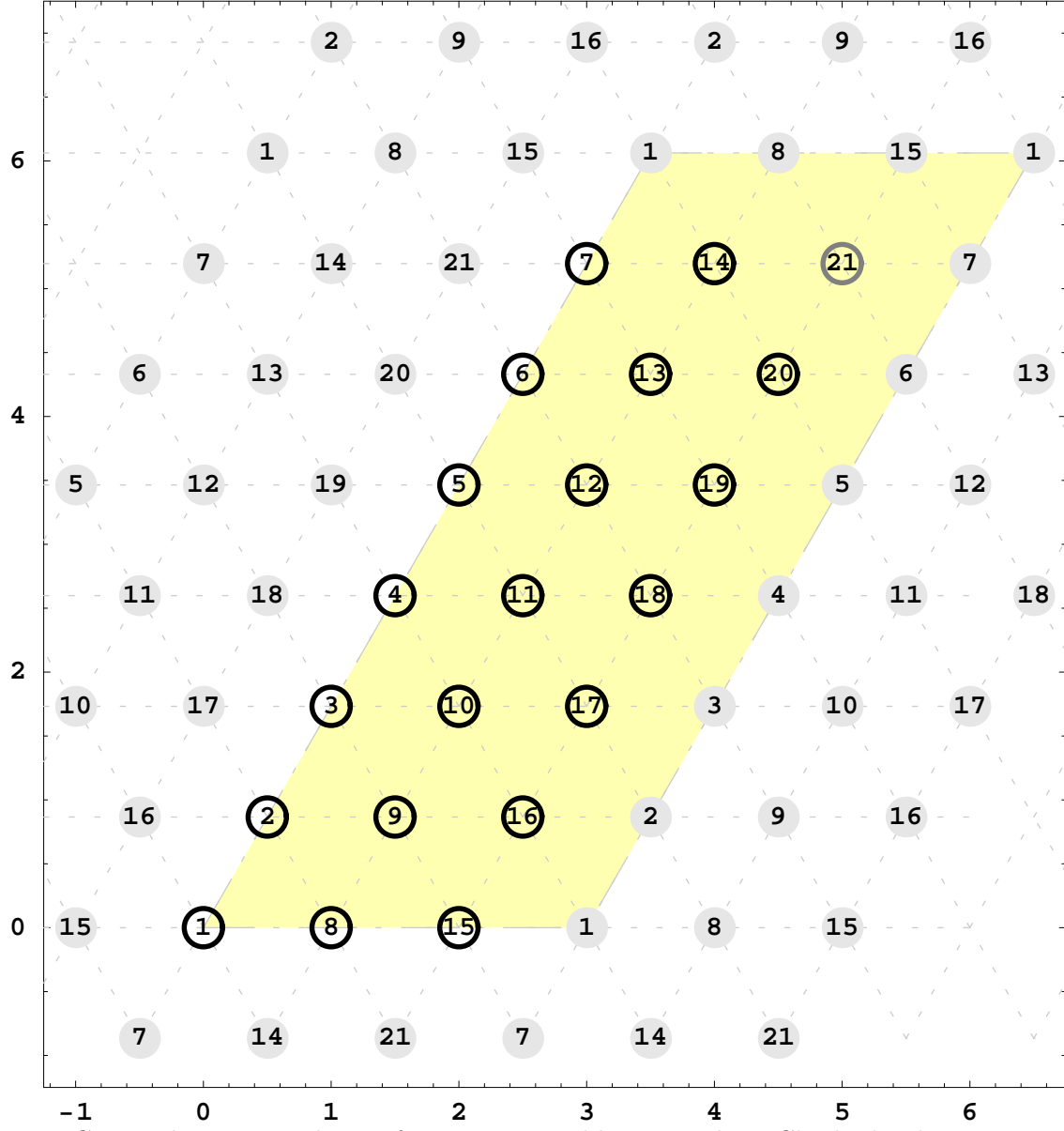


FIG. 6. The 21 site cluster frustrating 3-sublattice order. Check this by moving along the direction 1,2,3,... and placing 3 alternating classical Néel spins on consecutive sites, when arriving at the boundary a discontinuity arises.

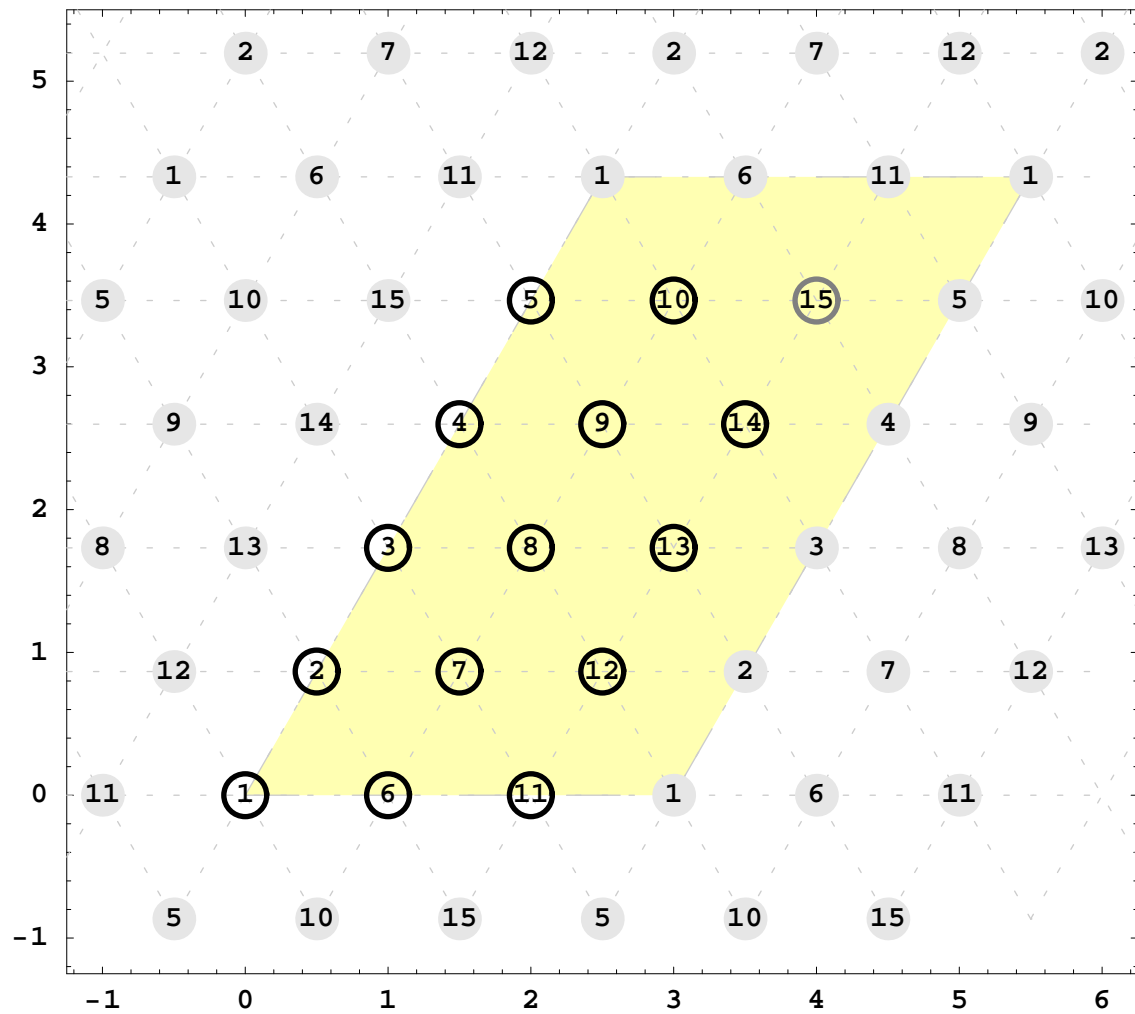


FIG. 7. The 15 site frustrated cluster